Schizophrenia Bulletin vol. 47 no. 1 pp. 31–43, 2021
doi:10.1093/schbul/sbaa090
Advance Access publication 4 July 2020

Hyperactive ACC-MDT Pathway Suppresses Prepulse Inhibition in Mice

Yangsik Kim*[,1–3], Young Woo Noh[4], Kyungdeok Kim[4], and Eunjoon Kim[3,4]

[1]Mental Health Research Institute, National Center for Mental Health, Seoul, South Korea; [2]Graduate School of Medical Science and Engineering, Korea Advanced Institute of Science and Technology, Daejeon, South Korea; [3]Center for Synaptic Brain Dysfunction, Institute for Basic Science, Daejeon, South Korea; [4]Department of Biological Science, Korea Advanced Institute of Science and Technology, Daejeon, South Korea

*To whom correspondence should be addressed; Mental Health Research Institute, National Center for Mental Health, Yongmasan-ro 127, Gwangjin-gu, Seoul, South Korea 04933; tel: +82-2-2204-0502, fax: +82-2-2204-0393, e-mail: medicusys@gmail.com

Altered prepulse inhibition (PPI) is an endophenotype associated with multiple brain disorders, including schizophrenia. Circuit mechanisms that regulate PPI have been suggested, but none has been demonstrated through direct manipulations. IRSp53 is an abundant excitatory postsynaptic scaffold implicated in schizophrenia, autism spectrum disorders, and attention-deficit/hyperactivity disorder. We found that mice lacking IRSp53 in cortical excitatory neurons display decreased PPI. IRSp53-mutant layer 6 cortical neurons in the anterior cingulate cortex (ACC) displayed decreased excitatory synaptic input but markedly increased neuronal excitability, which was associated with excessive excitatory synaptic input in downstream mediodorsal thalamic (MDT) neurons. Importantly, chemogenetic inhibition of mutant neurons projecting to MDT normalized the decreased PPI and increased excitatory synaptic input onto MDT neurons. In addition, chemogenetic activation of MDT-projecting layer 6 neurons in the ACC decreased PPI in wild-type mice. These results suggest that the hyperactive ACC-MDT pathway suppresses PPI in wild-type and IRSp53-mutant mice.

Key words: prepulse inhibition/mediodorsal thalamus/IRSp53/DREADD/schizophrenia/anterior cingulate cortex

Introduction

Prepulse inhibition (PPI) refers to an attenuated response to a startling stimulus in the presence of a non-startling prepulse.[1,2] Altered PPI has been observed in various psychiatric and neurological disorders, including schizophrenia, obsessive-compulsive disorder, autism spectrum disorders, Tourette's syndrome, Parkinson's disease, Huntington's disease, and Alzheimer's disease.[1,3–7] However, whether altered PPI is pathophysiologically associated with these diseases remains unclear; instead, PPI has been suggested as an endophenotype of the diseases and useful for monitoring related drug responses.[2]

PPI involves multiple brain regions, including the medial prefrontal cortex (mPFC), striatum, globus pallidus, thalamus, amygdala, habenula, and ventral tegmental area.[8,9] Conserved neural circuits have also been identified in animal models with altered PPI.[10–13] However, the operation of these PPI-related neural circuits has not been demonstrated through their direct modulation of a specific circuit using optogenetics or chemogenetics.[14–16]

The mediodorsal thalamus (MDT) is a higher-order thalamic nucleus that does not directly receive sensory inputs but is thought to relay sensory information to the cortex and facilitate reciprocal and mutual communication with the PFC.[17,18] Indeed, in rodents, the mPFC is generally defined by the prefrontal areas that are reciprocally connected with the MDT.[19,20] The MDT in rodents receives inputs mainly from layers 6 and 5 of the PFC and provides thalamocortical inputs to multiple prefrontal cortices, including the mPFC. Here, layers 3, 5, and 6 are major targets of the MDT, and layer 6 sends projections back to the MDT to provide reciprocal communication.[21]

Functionally, the MDT has been suggested to promote memory and cognition by reciprocally communicating with the PFC and supporting cortical functions.[22] For instance, decreasing connectivity between the MDT and PFC through chemogenetic inhibition of MDT neurons suppresses prefrontal cognitive tasks involving reversal learning and working memory, and beta-range synchrony between MDT and PFC.[23,24] In addition, pathway-specific MDT inhibition using optogenetic modulation has revealed a novel role for the MDT in the maintenance of prefrontal activity during working memory tasks.[25] Moreover, decreased functional coupling between the MDT and PFC has been linked to schizophrenia.[26,27]

© The Author(s) 2020. Published by Oxford University Press on behalf of the Maryland Psychiatric Research Center.
All rights reserved. For permissions, please email: journals.permissions@oup.com

Despite these extensive anatomical and functional associations of the MDT with the PFC, and the known participation of the PFC and MDT in PPI regulation,[8] it remains unclear how bidirectional PFC-MDT pathways, which are known to involve mainly excitatory synaptic transmissions,[21,28,29] regulate PPI. In addition, it is unclear how other excitatory and inhibitory inputs onto MDT neurons, eg, from subcortical regions such as the pallidum and substantia nigra,[18,30] regulate PPI.

IRSp53 (insulin receptor substrate protein of 53 kDa, also known as BAIAP2) is a scaffolding protein expressed in various brain regions that is mainly targeted to postsynaptic density (PSD) structures,[31,32] which represent electron-dense, multiprotein complexes that coordinate excitatory synapse development, function, and plasticity.[33–35] IRSp53 directly interacts with PSD-95,[36,37] an abundant excitatory postsynaptic scaffolding protein enriched in PSDs, and is thought to regulate actin filaments, the main cytoskeletal component of dendritic spines, by coordinating Rac/Cdc42-dependent actin polymerization.[32,38] IRSp53 has been implicated in multiple brain disorders, including schizophrenia,[39,40] autism spectrum disorders,[41–43] and attention-deficit/hyperactivity disorder.[44,45] In addition, mice lacking IRSp53 have been shown to display various behavioral and synaptic phenotypes, including excessive NMDA receptor function, as well as social deficits and cognitive impairments.[46,47]

In the present study, we found that mice with an IRSp53 deletion in cortical excitatory neurons exhibit decreased PPI as well as reduced excitatory synaptic input onto layer 6 cortical neurons in the anterior cingulate cortex (ACC), a brain region that reciprocally communicates with MDT,[22] but shows markedly increased intrinsic excitability of these neurons. These changes were associated with increased excitatory synaptic input onto MDT neurons lying downstream of the ACC. Importantly, chemogenetic inhibition of the neurons that project to MDT using a DREADD (designer receptor exclusively activated by designer drugs) approach normalized the decreased PPI and abnormally increased excitatory synaptic input onto MDT neurons in these mutant mice. In addition, chemogenetic activation of MDT-projecting neurons in the ACC in wild-type (WT) mice decreased PPI.

Methods

Animals

Mice were provided ad libitum access to food and water, and 3–4 mice were housed together in a cage under a 12-hour light-dark cycle. Mice were bred and maintained according to the Requirements of Animal Research at KAIST, and all procedures were approved by the Committee of Animal Research at KAIST (KA201). There were no differences in body weights among groups of age-matched mice. WT and IRSp53-mutant mice were identified by PCR genotyping using the following PCR primers: IRSp53 flox, AGGAGGTGTTTCTGCTCTGG/AATAGCAGTCTGGGGTCTGG; Cre, CGTACTGACGGTGGGAGAAT/TGCATGATCTCCGGTATTGA.

Statistical Analysis

Statistical analyses were performed using Prism 8 (GraphPad). Data normality was determined using the Shapiro-Wilk normality test. Normally distributed data were analyzed using Student's *t*-test and analysis of variance (ANOVA), followed by post hoc tests. Data failing the normality test were analyzed using Mann-Whitney and Kruskal-Wallis tests, followed by post hoc tests. The ROUT method was used to exclude outliers, based on a Q coefficient of 1%. Specific numbers of mice used and statistical details are shown in supplementary table S1.

Results

Decreased PPI in Mice Carrying an IRSp53 Deletion Restricted to Dorsal Telencephalic Excitatory Neurons

Because the cortex is one of the key brain regions that regulate PPI in mice[8] and IRSp53 is mainly expressed in excitatory neurons in the cortex,[31] we first generated mice carrying an IRSp53 deletion restricted to dorsal telencephalic excitatory neurons by crossing *Irsp53*$^{fl/fl}$ mice (floxed exons 4–6) with *Emx1-Cre* mice (Jax005628) (figure 1A).[48]

These mutant mice, designated *Emx1-Cre;Irsp53*$^{fl/fl}$, drove broad gene expression in cortical layers, as shown by crossing them with the tdTomato reporter mouse line and visualizing tdTomato signals in the brain (supplementary figure S1A). In addition, *Emx1-Cre;Irsp53*$^{fl/fl}$ mice showed substantially decreased levels of IRSp53 protein in the brain, as assessed by immunoblot analysis of whole-brain lysates (16 ± 1% of WT levels) (supplementary figures S1B and S1C).

In the PPI test, *Emx1-Cre;Irsp53*$^{fl/fl}$ mice showed a strong reduction in PPI without a change in general acoustic startle responses (figures 1B and 1C), suggesting that dorsal telencephalic *Irsp53* expression is important for normal PPI. Control mice carrying the *Emx1-Cre* allele without the *Irsp53*$^{fl/fl}$ allele showed normal levels of PPI (figure 1D). Decreased PPI in *Emx1-Cre;Irsp53*$^{fl/fl}$ mice, compared with control (*Irsp53*$^{fl/fl}$) mice, were still observed after eliminating the top decile of the control group and the bottom decile of *Emx1-Cre;Irsp53*$^{fl/fl}$ mice, for adjusting decreased startle magnitude tendency in *Emx1-Cre;Irsp53*$^{fl/fl}$ mice (supplementary figure S1D).

In behavioral tests, *Emx1-Cre;Irsp53*$^{fl/fl}$ mice showed modestly increased locomotor activity but normal anxiety-like behavior (figures 1E and 1F; supplementary figures S1E and S1F), which also were observed in the previous study.[49] These results collectively suggest that *Irsp53* deletion restricted to dorsal telencephalic excitatory neurons leads to decreased PPI in mice.

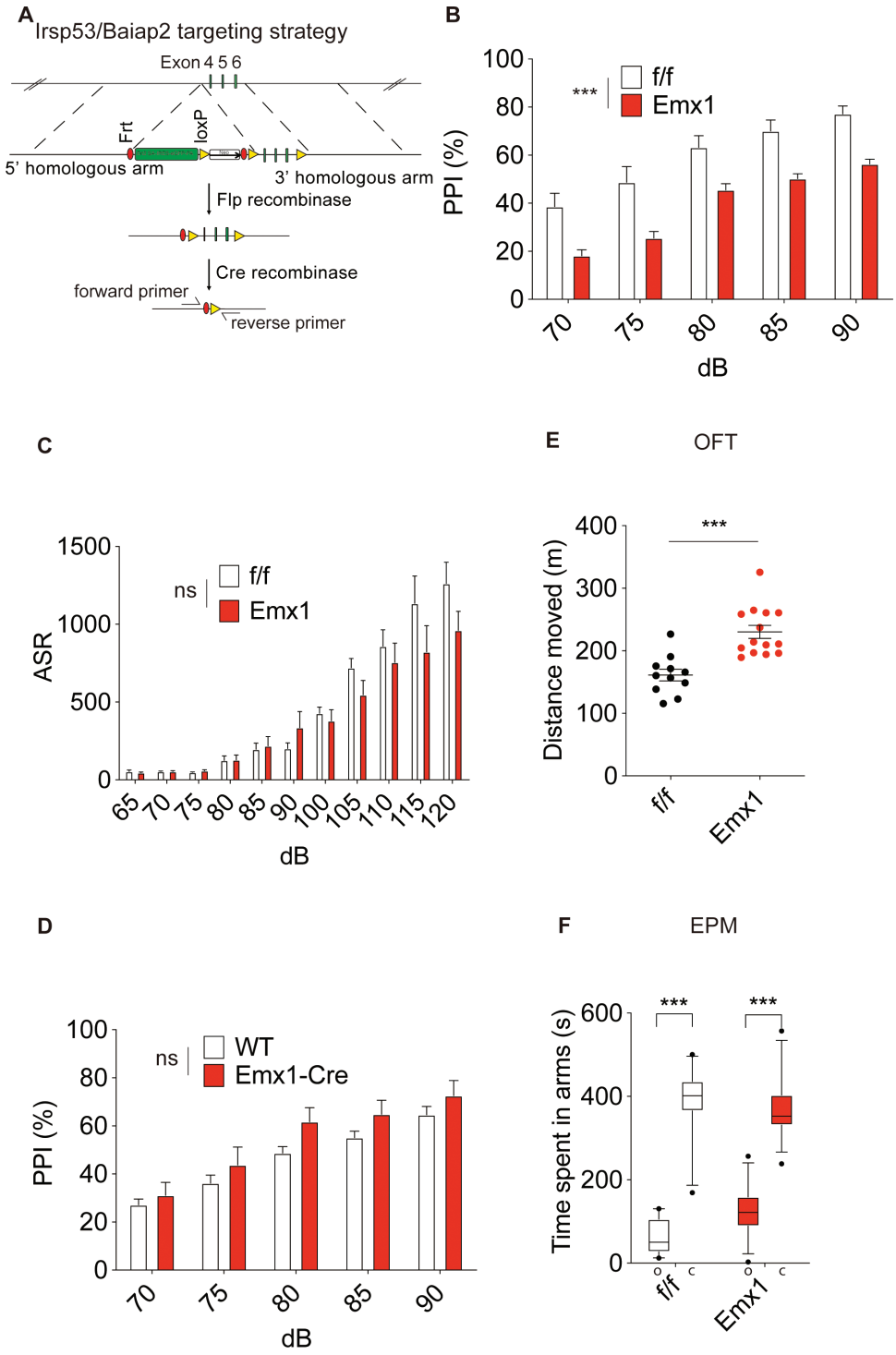

Fig. 1. Decreased prepulse inhibition (PPI) in mice carrying an IRSp53 deletion restricted to dorsal telencephalic excitatory neurons and layer 6 pyramidal neurons. (A) Strategy for the generation of *Emx1-Cre;Irsp53*$^{fl/fl}$ mice. Exons 4–6 of the Irsp53 (*Baiap2*) gene in mice were floxed to allow for Cre recombinase-mediated deletion of Irsp53. (B) Decreased PPI in *Emx1-Cre;Irsp53*$^{fl/fl}$ mice, compared with control (*Irsp53*$^{fl/fl}$) mice; $n = 11$ mice for control (Irsp53$^{fl/fl}$) and 14 for *Emx1-Cre;Irsp53*$^{fl/fl}$; $^{***}P < .001$, 2-way ANOVA with Bonferroni's test. (C) Normal levels of acoustic startle responses (ASR) in *Emx1-Cre;Irsp53*$^{fl/fl}$ mice compared with control (*Irsp53*$^{fl/fl}$) mice; $n = 8$ mice for control (Irsp53$^{fl/fl}$) and 8 for *Emx1-Cre;Irsp53*$^{fl/fl}$; ns, not significant; 2-way ANOVA with Bonferroni's test. (D) Normal levels of PPI in control *Emx1-Cre* mice lacking the *Irsp53*$^{fl/fl}$ allele compared with control (wild-type [WT] C57BL/6J) mice; $n = 8$ mice for WT and 8 for Emx1-Cre; ns, not significant; 2-way ANOVA with Bonferroni's test. (E) Increased locomotor activity of *Emx1-Cre;Irsp53*$^{fl/fl}$ mice in the open-field test; $n = 11$ mice for control (Irsp53$^{fl/fl}$), 14 for *Emx1-Cre;Irsp53*$^{fl/fl}$, $^{***}P < .001$, Student's *t*-test. (F) Normal anxiety-like behavior of *Emx1-Cre;Irsp53*$^{fl/fl}$ mice in the elevated plus-maze test compared with control (*Irsp53*$^{fl/fl}$) mice. O, open arms; C, closed arms; $n = 11$ mice for control (Irsp53$^{fl/fl}$), 14 for *Emx1-Cre;Irsp53*$^{fl/fl}$; $^{***}P < .001$, 2-way ANOVA with Bonferroni's test.

Next, c-Fos staining was used to observe neuronal activities in the basal status on mPFC including ACC (supplementary figures S1G and S1H). *Emx1-Cre;Irsp53*$^{fl/fl}$ mice showed suppressed c-Fos activities in mPFC compared with control mice.

Decreased Excitatory Synaptic Transmission, but Strongly Increased Neuronal Excitability, in ACC Layer 6 Pyramidal Neurons in Emx1-Cre;Irsp53$^{fl/fl}$ Mice

Because layer 6 PFC neurons and their reciprocal communication with MDT neurons have been implicated higher brain functions,[22–25] and the functional coupling between PFC and MDT has been associated with schizophrenia[26,27] and PPI regulation,[8] we tested if layer 6 cortical neurons in the ACC region of *Emx1-Cre;Irsp53*$^{fl/fl}$ mice display altered synaptic and neuronal functions.

The frequency, but not amplitude, of miniature excitatory postsynaptic currents (mEPSCs) in ACC layer 6 pyramidal neurons, which can be identified by their layer location as well as their unique electrophysiological properties,[50] was significantly decreased in *Emx1-Cre;Irsp53*$^{fl/fl}$ mice compared with control mice (*Irsp53*$^{fl/fl}$ alone without Cre expression) (figure 2A), in line with the reported requirement of IRSp53 for the maintenance of excitatory synapses in the mPFC.[47] In contrast, miniature inhibitory postsynaptic currents (mIPSCs) were normal in both control and *Emx1-Cre;Irsp53*$^{fl/fl}$ mice (figure 2A).

Because the defects in synaptic proteins often induce changes in the intrinsic neuronal properties of neurons,[51] we next measured the excitability of ACC layer 6 pyramidal neurons in *Emx1-Cre;Irsp53*$^{fl/fl}$ mice. Intriguingly, the excitability of ACC layer 6 pyramidal neurons was strongly increased in *Emx1-Cre;Irsp53*$^{fl/fl}$ mice compared with that in control mice (*Irsp53*$^{fl/fl}$), as shown by the current-firing curve, action potential threshold, and input resistance (figures 2B–D). These results suggest that *Irsp53* deletion in dorsal telencephalic excitatory neurons suppresses excitatory synaptic input onto these neurons, but markedly increases their intrinsic excitability, likely altering their output functions.

Increased Excitatory Synaptic Input Onto MDT Neurons in Emx1-Cre;Irsp53$^{fl/fl}$

Given the possibility that *Irsp53* deletion in layer 6 cortical neurons might alter the output functions of these neurons, we next measured excitatory synaptic input onto downstream target neurons in the MDT, a brain region known to receive synaptic inputs from major cortical and subcortical brain regions, including deep (layer 5/6) cortical layers in the PFC.[18]

Intriguingly, the frequency, but not amplitude, of mEPSCs in MDT neurons was significantly increased in *Emx1-Cre;Irsp53*$^{fl/fl}$ mice compared with control (*Irsp53*$^{fl/fl}$) MDT neurons (figure 3A). Notably, mIPSC frequency was also increased in control and *Emx1-Cre;Irsp53*$^{fl/fl}$ mice (figure 3A), indicative of a parallel increase in excitatory and inhibitory synaptic input onto MDT neurons. The excitability of MDT neurons was largely normal in *Emx1-Cre;Irsp53*$^{fl/fl}$ mice, as shown by normal current-firing curve and input resistance, although action potential threshold was increased, indicative of a modest decreased in neuronal excitability (figures 3B–D). These results suggest that *Irsp53* deletion in dorsal telencephalic excitatory neurons increases excitatory synaptic input onto MDT neurons and induces a parallel increase in inhibitory synaptic input, without causing strong changes in the excitability of the mutant MDT neurons.

Chemogenetic Inhibition of MDT and MDT-Projecting Neurons Using the DREADD Approach Normalizes PPI in Emx1-Cre;Irsp53$^{fl/fl}$ Mice

The increased excitatory synaptic input onto MDT neurons in *Emx1-Cre;Irsp53*$^{fl/fl}$ mice mentioned above would increase the output function of these neurons. This could be compensated by other changes such as an increase in inhibitory synaptic input onto MDT neurons, as suggested by the mE/IPSC results (figure 3A). However, excitatory and inhibitory synaptic inputs in the presence of network activity, measured by spontaneous excitatory synaptic transmission (sEPSCs), indicated a strong increase in the ratio of synaptic excitation/inhibition in mutant MDT neurons (see below). If this increase in excitatory synaptic input induces a decrease in PPI in *Emx1-Cre;Irsp53*$^{fl/fl}$ mice, then suppressing the activity of MDT neurons may normalize the PPI phenotype of mutant mice.

To this end, we sought to suppress the activity of MDT neurons using chemogenetic inhibition (hM4Di) in the DREADD system, a modified version of the human M4 muscarinic receptor that is activated by the inert clozapine metabolite clozapine-N-oxide (CNO).[52–54]At the same time, we wanted to suppress the activity of neurons projecting to the MDT (MDT-projecting neurons) to prevent the chemogenetic inhibition of MDT neurons from being influenced by excitatory and inhibitory synaptic inputs onto MDT neurons. We thus used a retrograde chemogenetic inhibition strategy in the MDT, which would drive not only the retrograde expression of hM4Di in MDT-projecting neurons but also the anterograde expression of hM4Di in local MDT neurons through cell body infection. Specifically, we injected an adeno-associated virus (AAV), AAVrg-hSyn-hM4Di-mCherry viral expression construct into the MDT region of postnatal week 8 *Emx1-Cre;Irsp53*$^{fl/fl}$ mice to retrogradely express hM4Di in upstream MDT-projecting neurons and anterogradely express hM4Di in local MDT neurons, and then performed behavioral and electrophysiological experiments at 14 and 16 weeks, respectively (figures 4A and 4B).

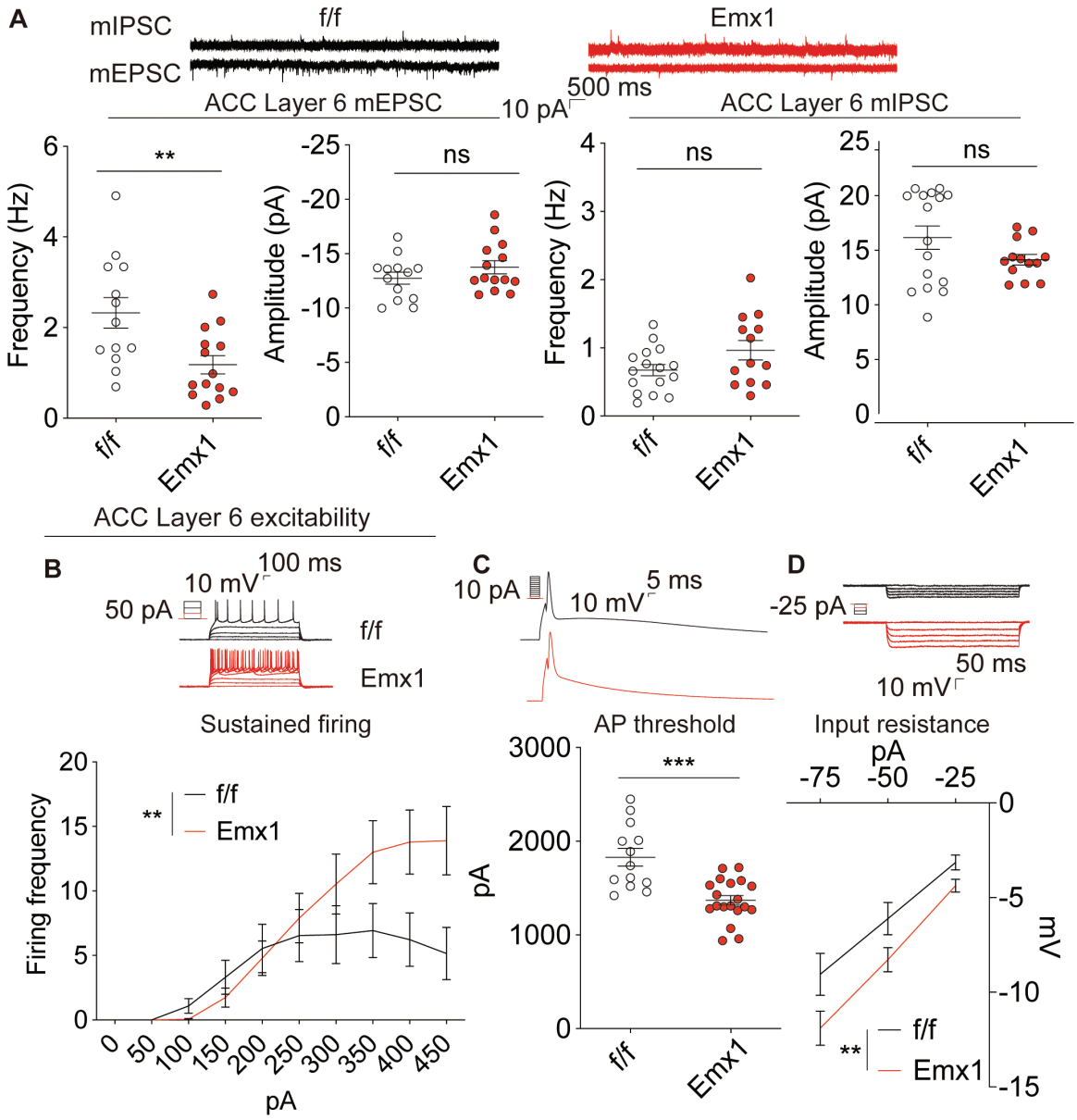

Fig. 2. Decreased excitatory synaptic transmission, but markedly increased neuronal excitability, in layer 6 pyramidal neurons in the anterior cingulate cortex (ACC) in *Emx1-Cre;Irsp53*$^{fl/fl}$ mice. (A) Decreased frequency of miniature excitatory postsynaptic currents (mEPSCs), but normal miniature inhibitory postsynaptic currents (mIPSCs), in layer 6 pyramidal neurons in the ACC of *Emx1-Cre;Irsp53*$^{fl/fl}$ mice compared with control (*Irsp53*$^{fl/fl}$) mice (2 months). mEPSC, $n = 13$ neurons from 3 mice for control (f/f) and 14, 3 for Emx1-Cre; mIPSC, $n = 16$, 4 mice for control (f/f) and 13, 3 for Emx1-Cre; $^{**}P < .01$; ns, not significant; Student's *t*-test. (B–D) Increased excitability of layer 6 cortical neurons in the ACC of *Emx1-Cre;Irsp53*$^{fl/fl}$ mice compared with control (*Irsp53*$^{fl/fl}$) mice (2 months), as indicated by current-firing curve, action potential (AP) threshold, and input resistance. Note that the durations for the current injections differ between the experiments for b and c panels, 1 vs 10 msec, respectively. Sustained firing, $n = 13$ neurons from 3 mice for control (f/f), 19, 3 for Emx1-Cre, AP threshold, $n = 13$, 3 mice for control (f/f), 19, 3 for Emx1-Cre, Input resistance; $n = 10$, 3 mice for control (f/f), 18, 3 for Emx1-Cre; $^{**}P < .01$, $^{***}P < .001$, 2-way ANOVA with Bonferroni's test for sustained firing and input resistance, Student's *t*-test for AP threshold.

Successful retrograde expression of hM4Di-mCherry fusion proteins in MDT-projecting neurons was confirmed by the strong mCherry signals observed in the ACC as well as the insular cortex (supplementary figure S2A). The latter signals did not overlap with the latexin-positive claustrum (supplementary figure S2B), which is known to link the insular cortex and striatum to integrate and modulate multiple sensory inputs, similar to the MDT.[55,56] In addition, we could observe strong mCherry signals in the MDT, which could represent hM4Di-mCherry expression in local MDT neurons as well as at nerve terminals attached to MDT neurons.

Based on the strong mCherry signals in the insular cortex, we performed additional electrophysiological experiments

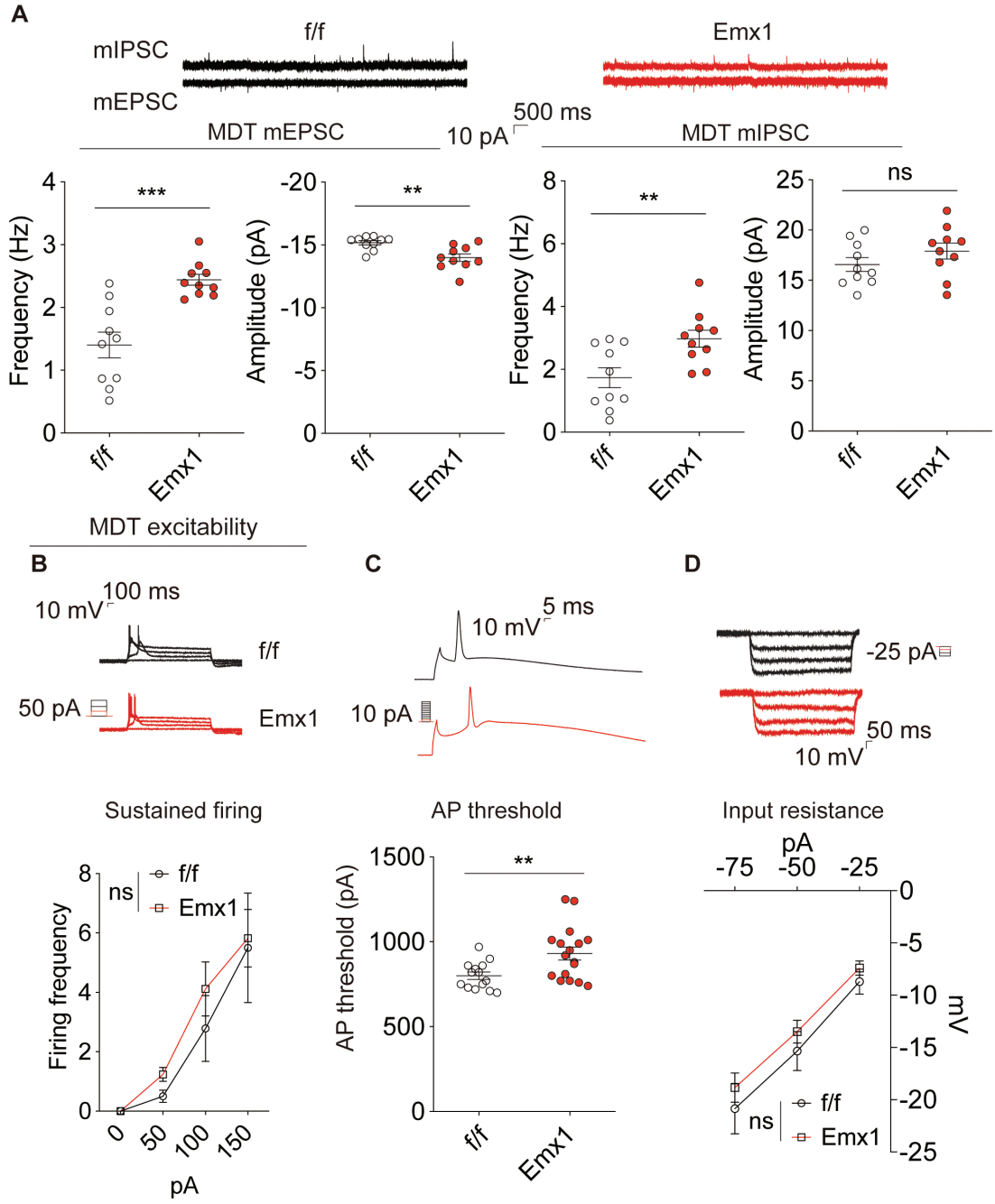

Fig. 3. Increased excitatory synaptic input and moderately decreased neuronal excitability in mediodorsal thalamic (MDT) neurons in *Emx1-Cre;Irsp53*$^{fl/fl}$ mice. (A) Increased frequency of miniature excitatory postsynaptic currents (mEPSCs) and miniature inhibitory postsynaptic currents (mIPSCs) in MDT neurons in *Emx1-Cre;Irsp53*$^{fl/fl}$ mice compared with control (*Irsp53*$^{fl/fl}$) mice. mEPSC, $n = 10$ neurons from 3 mice for control (f/f), 10, 3 for Emx1-Cre; mIPSC, $n = 10$ neurons from 3 mice for control (f/f), 10, 3 for Emx1-Cre; $^{**}P < .01$, $^{***}P < .001$; ns, not significant, Student's *t*-test. (B–D) Moderately decreased neuronal excitability in MDT neurons in *Emx1-Cre;Irsp53*$^{fl/fl}$ mice (2 months), as shown by normal current-firing curve and input resistance but increased action potential threshold; $n = 17$ neurons from 3 mice for control (f/f) and 14, 3 for Emx1-Cre, AP threshold, $n = 17$, 3 mice for control (f/f) and 14, 3 for Emx1-Cre, Input resistance, $n = 17$, 3 mice for control (f/f) and 14, 3 for Emx1-Cre; $^{**}P < .01$; ns, not significant, 2-way ANOVA with Bonferroni's test for sustained firing and input resistance, Student's *t*-test for AP threshold.

and found that excitatory synaptic transmission in layer 5 pyramidal neurons in the insular cortex of *Emx1-Cre;Irsp53*$^{fl/fl}$ mice was suppressed, as shown by a decrease in the frequency of sEPSCs (supplementary figure S3A), similar to the results obtained from ACC layer 5 pyramidal neurons in *Emx1-Cre;Irsp53*$^{fl/fl}$ mice (figure 2A). In contrast, intrinsic excitability was normal in *Emx1-Cre;Irsp53*$^{fl/fl}$ insular cortex layer 5 pyramidal neurons (supplementary figures S3B–D), unlike the increase observed in the mutant ACC neurons (figure 2B). These results suggest that the output function

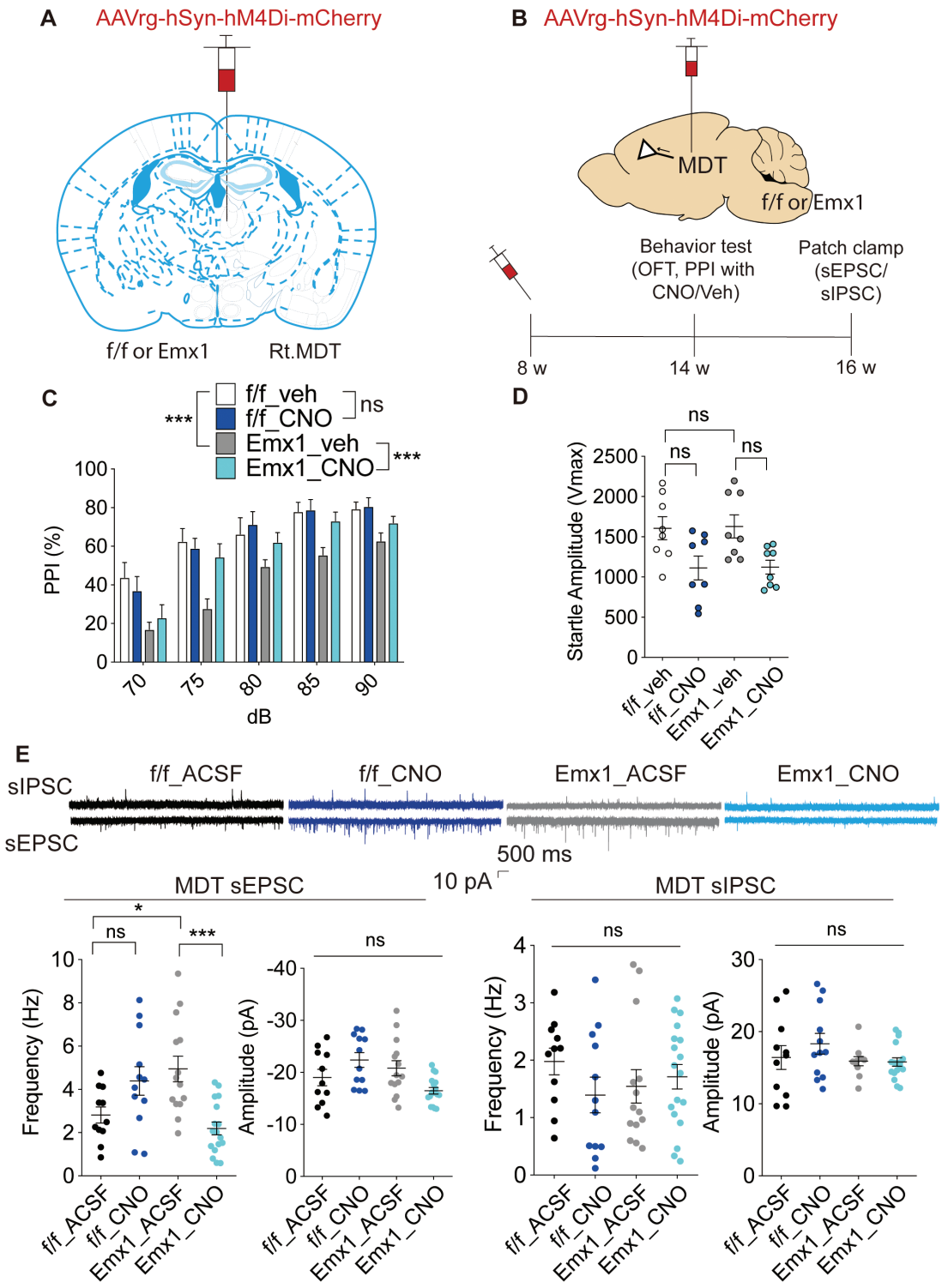

Fig. 4. Chemogenetic inhibition of mediodorsal thalamic (MDT) and MDT-projecting neurons using the DREADD (designer receptor exclusively activated by designer drugs) approach normalizes the decreased prepulse inhibition (PPI) and increased excitatory synaptic input onto MDT neurons in *Emx1-Cre;Irsp53*$^{fl/fl}$ mice. (A–B) Experimental scheme for testing the effects of chemogenetic inhibition of MDT and MDT-projecting neurons on PPI. AAVrg-hSyn-hM4Di-mCherry was injected into the MDT region of *Emx1-Cre;Irsp53*$^{fl/fl}$ and control (*Irsp53*$^{fl/fl}$) mice (8 weeks), followed by behavioral experiments (open-field test and PPI in the presence of CNO/vehicle injected [i.p.] 30 min prior to behavioral experiments) at 14 weeks and sE/IPSC measurements at 18 weeks. Note that hM4Di-mCherry proteins are anterogradely expressed in local MDT neurons and also retrogradely expressed in all neurons that provide synaptic input onto MDT neurons, although major mCherry signals were detected in the anterior cingulate cortex (ACC) and insular cortex. (C) Normalization of the decreased PPI in *Emx1-Cre;Irsp53*$^{fl/fl}$ mice by CNO-dependent chemogenetic inhibition of MDT neurons and MDT-projecting neurons that retrogradely express hM4Di proteins; n = 8 mice for control (f/f) + vehicle, 8 for control (f/f) + CNO (4i), 8 for Emx1 +

of *Emx1-Cre;Irsp53*$^{fl/fl}$ neurons in the insular cortex is less likely to be increased and provide increased excitatory input onto MDT neurons.

Injection of *Emx1-Cre;Irsp53*$^{fl/fl}$ mice with CNO (2.5 mg/kg, ip) 1 hour prior to the measurement of PPI normalized the decreased PPI in *Emx1-Cre;Irsp53*$^{fl/fl}$ mice, yielding values comparable to those in control, vehicle-treated *Emx1-Cre;Irsp53*$^{fl/fl}$ mice (figures 4C–E). This chemogenetic inhibition, however, had no effect on the locomotor activity of *Emx1-Cre;Irsp53*$^{fl/fl}$ mice in the open-field test (supplementary figure S4A). In a control experiment, administration of CNO by itself to *Emx1-Cre;Irsp53*$^{fl/fl}$ and *Irsp53*$^{fl/fl}$ mice, which do not express hM4Di, had no effect on PPI (supplementary figure S4B). In addition, hM4Di retrogradely transported to layer 6 pyramidal neurons in the ACC strongly suppressed neuronal firing events, as expected (supplementary figures S4C and S4D).

To avoid concerns about clozapine conversion of the CNO,[54] we performed further PPI experiments using clozapine and another antipsychotics haloperidol. Thirty minutes after clozapine administration (2.5 mg/kg, ip), PPI is increased in both control and *Emx1-Cre;Irsp53*$^{fl/fl}$ mice. In contrast to clozapine, PPI is decreased in control but not in *Emx1-Cre;Irsp53*$^{fl/fl}$ mice after haloperidol injection (supplementary figures S5A–D). In addition, liquid chromatography/mass spectrometer (LC/MS) was measured for neurotransmitters such as dopamine and serotonin (5-HT) in whole-brain extracts. *Emx1-Cre;Irsp53*$^{fl/fl}$ mice showed that decreased serotonin level compared with the control. Comparing neurotransmitter level between the vehicle and CNO group of WT mice, the 2 groups did not show a difference (supplementary figures S5E–H).

Chemogenetic Inhibition of MDT and MDT-Projecting Neurons Using the DREADD Normalizes the Increased Excitatory Synaptic Input Onto MDT Neurons in Emx1-Cre;Irsp53$^{fl/fl}$ Mice

We next tested whether the normalization of PPI in *Emx1-Cre;Irsp53*$^{fl/fl}$ mice by chemogenetic inhibition of MDT and MDT-projecting neurons is associated with changes in excitatory synaptic input onto MDT neurons. Here, we measured sEPSCs rather than mEPSCs, because network activity should be allowed to be able to observe CNO-dependent changes in synaptic input onto MDT neurons. It should be noted that synaptic transmission measured in *Emx1-Cre;Irsp53*$^{fl/fl}$ MDT neurons in coronal slice preparations is largely disconnected from MDT-projecting neuronal cell bodies remote from the MDT (ie, in the frontal cortex), although hM4Di proteins targeted to the nerve terminals attached to MDT neurons, mentioned above, should be able to suppress presynaptic neurotransmitter release independent of neuronal activity.[57–59]

Intriguingly, under basal conditions (in the absence of CNO treatment), sEPSC frequency, but not amplitude, was increased in *Emx1-Cre;Irsp53*$^{fl/fl}$ MDT neurons compared with control (*Irsp53*$^{fl/fl}$) MDT neurons (figure 4E), similar to mEPSC results (figure 3A). In contrast, sIPSC frequency in *Emx1-Cre;Irsp53*$^{fl/fl}$ MDT neurons was comparable to that of control (*Irsp53*$^{fl/fl}$) MDT neurons (figure 4E), dissimilar to the increased mIPSC frequency in the mutant neurons (figure 3A). These results suggest that the increased inhibitory, but not excitatory, synaptic transmission in *Emx1-Cre;Irsp53*$^{fl/fl}$ MDT neurons was suppressed by network activity and that the output function of these MDT neurons is likely to be increased.

More importantly, the abnormally increased sEPSC frequency was normalized by treatment of hM4Di-expressing *Emx1-Cre;Irsp53*$^{fl/fl}$ slices with CNO; however, CNO had no effect on sEPSCs in control (*Irsp53*$^{fl/fl}$) slices (figure 4E). In addition, CNO treatment had no effect on sIPSCs in hM4Di-expressing *Emx1-Cre;Irsp53*$^{fl/fl}$ or control (*Irsp53*$^{fl/fl}$) slices (figure 4E). These results suggest that the chemogenetic inhibition normalizes the abnormally increased excitatory synaptic input onto *Emx1-Cre;Irsp53*$^{fl/fl}$ MDT neurons, likely by acting on hM4Di-containing nerve terminals.

Chemogenetic Activation but Not Inhibition of the ACC-MDT Pathway Decreases PPI in WT Mice

The results described thus far do not provide evidence on whether any specific groups of MDT-projecting cortical neurons are important for PPI modulation. To address this question, we initially sought to combine retrograde AAV constructs carrying DIO-hM4Di injected into MDT and Cre-dependent hM4Di expression in a specific group of cortical neurons such as MDT-projecting neurons in the ACC. However, this approach was not feasible in *Emx1-Cre;Irsp53*$^{fl/fl}$ mice because Emx1-driven Cre expression occurs in a large number of dorsal telencephalic excitatory neurons and would induce widespread hM4Di expression in various cortical layers. To

vehicle, and 8 for Emx1 + CNO (4i); ***$P < .001$, 2-way ANOVA with Bonferroni's test. (D) Normal levels of acoustic startle responses at 120 dB in *Emx1-Cre;Irsp53*$^{fl/fl}$ mice and control (*Irsp53*$^{fl/fl}$) mice treated with vehicle and CNO; $n = 8$ for control f/f_veh (vehicle), 8 for control f/f_CNO, 8 for Emx1_veh, and 8 for Emx1_CNO; ns, not significant, 1-way ANOVA with Bonferroni's test. (E) Normalization of the increased frequency of sEPSCs in MDT neurons from hM4Di-expressing *Emx1-Cre;Irsp53*$^{fl/fl}$ slices. Note that sEPSC frequency in *Emx1-Cre;Irsp53*$^{fl/fl}$ MDT neurons is higher than that in control (*Irsp53*$^{fl/fl}$) mice, similar to the mEPSC results, although sIPSC frequencies are similar in *Emx1-Cre;Irsp53*$^{fl/fl}$ MDT and control (*Irsp53*$^{fl/fl}$) neurons, dissimilar to the mIPSC results. sEPSC, $n = 11$ neuron from 3 mice for control f/f_ ACSF (artificial cerebrospinal fluid), 12, 3 for control f/f_CNO, 14, 3 for Emx1_ACSF, and 17, 3 for Emx1_CNO; sIPSC, $n = 11$ neuron from 3 mice for control f/f_ACSF, 12, 3 for control f/f_CNO, 14, 3 for Emx1_ACSF, and 18, 3 for Emx1_CNO; *$P < .05$, ***$P < .001$; ns, not significant, 1-way ANOVA with Bonferroni's test.

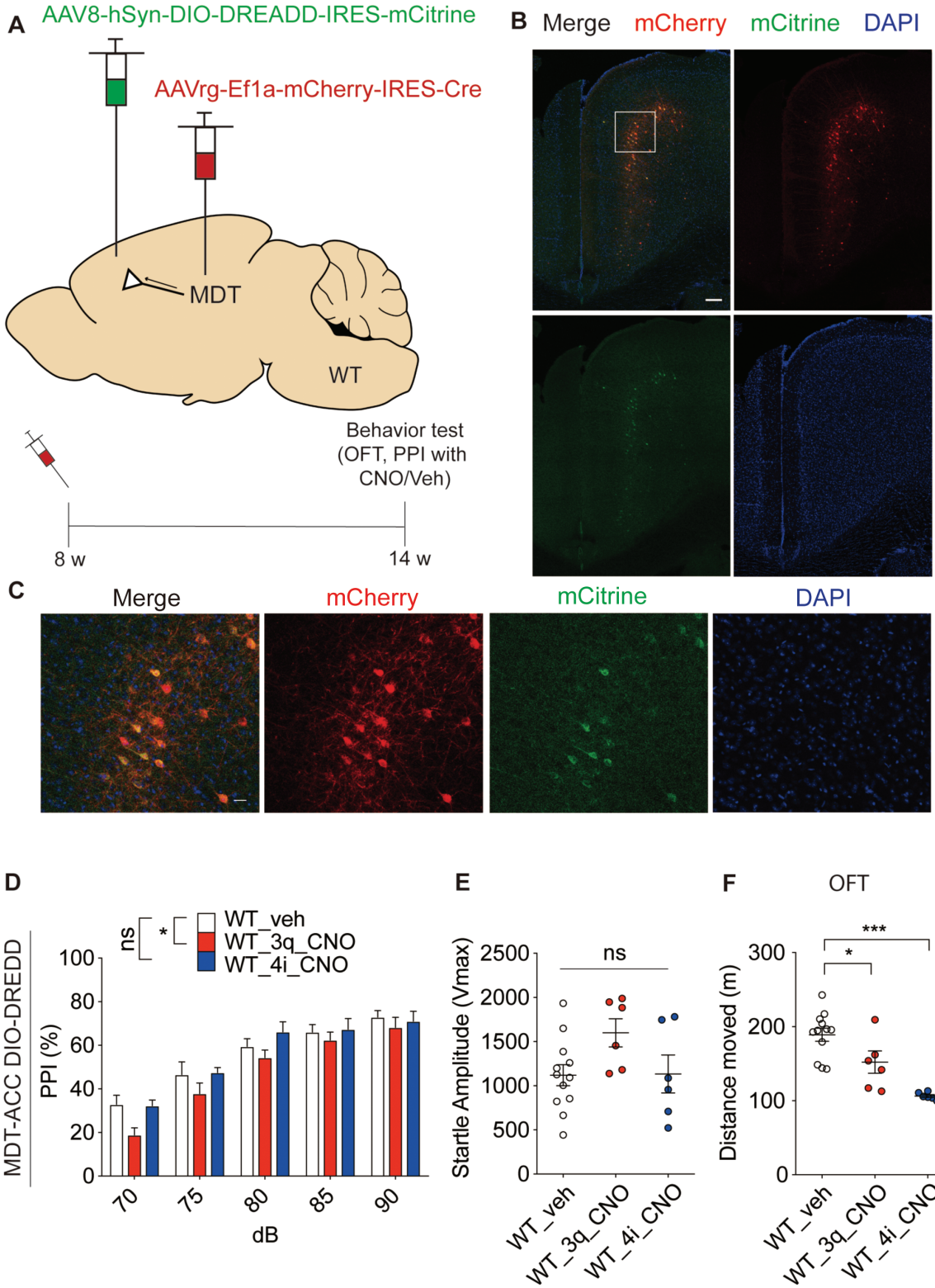

Fig. 5. Chemogenetic activation but not inhibition of the anterior cingulate cortex-mediodorsal thalamic (ACC-MDT) pathway decreases prepulse inhibition (PPI) in WT mice. (A) Experimental scheme for testing the effects of chemogenetic activation and inhibition MDT-projecting ACC neurons on PPI using a dual injection of AAV constructs in wild-type (WT) mice. Specifically, AAVrg-EF1a-mCherry-IRES-Cre was injected into the MDT region and AAV5-hSyn-DIO-DREADD (hM3Dq and hM4Di)-IRES-mCitrine was injected into the ACC in WT mice (8 weeks), followed by behavioral experiments (open-field test and PPI in the presence of CNO/vehicle injected [i.p.] 1 hr prior to behavioral experiments) at 14 weeks. For vehicle injection, the data from hM3Dq- and hM4Di-expressing mice were combined. (B and C) Strong colocalization of retrogradely expressed mCherry and locally expressed mCitrine in

circumvent this limitation, we attempted to use WT mice and inject AAVrg-EF1a-mCherry-internal ribosome entry site (IRES)-Cre into MDT and AAV5-hSyn-DIO-DREADD-IRES-mCitrine into ACC in parallel to drive hM3Dq or hM4Di expression in MDT-projecting ACC neurons by retrograde Cre expression (figures 5A and 5B). AAV injections and behavioral tests were performed at 8 and 14 weeks, respectively (figure 5A).

At 14 weeks, retrogradely expressed mCherry signals strongly colocalized with mCitrine in MDT-projecting ACC neurons mainly in deep cortical layers (figure 5C). Importantly, chemogenetic activation of MDT-projecting ACC neurons by CNO treatment induced a decrease in PPI in hM3Dq-expressing WT mice, whereas chemogenetic inhibition of MDT-projecting ACC neurons had no effect on PPI in hM4Di-expressing WT mice (figures 5D and 5E). Chemogenetic activation of MDT-projecting ACC neurons had no effect on the locomotor activity of WT mice in the open-field test, although chemogenetic inhibition of MDT-projecting ACC neurons induced a decrease in locomotor activity (figure 5F). These results suggest that PPI is decreased in WT mice by chemogenetic activation, but not inhibition, of MDT-projecting ACC neurons, which would increase excitatory, but not inhibitory, synaptic input onto MDT neurons.

Discussion

Our study revealed that IRSp53 deletion restricted to dorsal telencephalic excitatory neurons reduces PPI in mice (figure 1). Our study further provided insight into underlying synaptic mechanisms, demonstrating reduced excitatory synaptic transmission in layer 6 pyramidal neurons in the ACC (figure 2A). This finding is in line with the observation that IRSp53 is a core component of PSDs at excitatory synapses,[32] and previous study reports that IRSp53 is mainly expressed in glutamatergic excitatory neurons in cortical areas.[31]In addition, global IRSp53 KO in mice has been shown to cause a decrease in excitatory synaptic transmission and dendritic spine density in layer 2/3 pyramidal neurons in the prelimbic region of the mPFC.[47]

Unexpectedly, however, these decreases in excitatory synaptic transmission were associated with strongly increased excitability in layer 6 pyramidal neurons in the ACC but not in layer 5 pyramidal neurons in the insular cortex (figures 2B–D; supplementary figures S3B–D). It is possible that the decreased excitatory synaptic transmission might have induced a compensatory increase in neuronal excitability that serves to maintain a constant neuronal output, although an overshoot seems to have occurred in the case of the mutant ACC (not insular cortex), resulting in excessive neuronal excitability. In addition, a similar increase in neuronal excitability has been observed in mouse and human neurons that lack Shank3, an abundant excitatory postsynaptic scaffolding protein.[51] Moreover, mice in which the Arp2/3 complex subunit ArpC3, a critical regulator of actin filaments in excitatory synapses,[60,61] is deleted in excitatory neurons have been shown to display haloperidol-responsive schizophrenia-like behavioral abnormalities and progressively decreased dendritic spine density; paradoxically, however, these mice also exhibit increased excitatory synaptic transmission in a group of frontal cortical neurons that project to dopamine (DA) neurons in the midbrain ventral tegmental area (VTA) and substantia nigra regions, changes that lead to abnormal increases in locomotor activity and striatal DA levels.[62,63]

Consistent with the hypothesis that the increased excitability of layer 6 pyramidal neurons increases excitatory synaptic input onto MDT neurons, *Emx1-Cre;Irsp53*$^{fl/fl}$ MDT neurons showed an increase in excitatory synaptic input (figure 3A) that is only moderately corrected by network activities (figure 4E). The parallel increase in the frequency of mIPSCs in MDT neurons is also notable (figure 3A), although it was corrected by network activities (figure 4E). Because MDT neurons mainly receive excitatory, but not inhibitory, synaptic inputs from the PFC,[64] and local GABAergic neurons are rare in the MDT,[21] increased inhibitory synaptic input onto MDT neurons might involve in the increased function of cortical neurons that project to thalamic reticular nuclei (TRN) of the thalamic nucleus, which is known to be enriched for parvalbumin-positive neurons that project to MDT neurons.[17,18]

In further support of the hypothesis that increased excitatory synaptic input onto MDT neurons decreases PPI, chemogenetic inhibition of MDT and MDT-projecting neurons normalized PPI in *Emx1-Cre;Irsp53*$^{fl/fl}$ mice (figures 4C and 4D). Among many MDT-projecting neurons, frontal but not insular cortical neurons seem to be more important because frontal (not insular) cortical neurons displayed elevated excitability. In addition, among MDT-projecting neurons, excitatory rather than inhibitory neurons seem to be more important because chemogenetic inhibition

MDT-projecting neurons in ACC (14 weeks), indicative of Cre-dependent expression of mCitrine. Scale bar, 200 µm in C panels and 20 µm in D panels. (D) Chemogenetic activation but not inhibition of the ACC-MDT pathway decreases PPI in WT mice; $n = 12$ for WT_vehicle (3q + 4i), 6 for WT_CNO (3q), and 6 for WT_CNO (4i), $^*P < .05$; ns, not significant, 2-way ANOVA with Bonferroni's test. (E) Normal levels of acoustic startle responses at 120 dB in WT mice treated with vehicle and CNO; $n = 12$ for WT_vehicle (3q + 4i), 6 for WT_CNO (3q), and 6 for WT_CNO (4i); ns, not significant, 1-way ANOVA with Bonferroni's test. (F) Chemogenetic activation and inhibition of the ACC-MDT pathway decrease the locomotor activities in WT mice in the open-field test; $n = 12$ for WT_vehicle (3q + 4i), 6 for WT_CNO (3q), and 6 for WT_CNO (4i); $^*P < .05$, $^{***}P < .001$, 1-way ANOVA with Bonferroni's test.

substantially decreased excitatory synaptic input onto MDT neurons but had no effect on inhibitory synaptic input (figure 4E).

These results, however, do not provide a clear answer on which (cortical vs subcortical) MDT-projecting neurons are more important. Importantly, chemogenetic activation but not inhibition of MDT-projecting neurons in the ACC, which would increase excitatory synaptic input onto MDT neurons, decreases PPI in WT mice (figure 5). This suggests that the activation of the ACC-MDT pathway is sufficient to decrease PPI in WT mice, and, together with the results from *Emx1-Cre;Irsp53*$^{fl/fl}$ mice, that abnormally activated ACC-MDT pathway may underlie the decreased PPI in the mutant mice, although the roles of non-ACC-MDT pathway cannot be excluded.

Chemogenetics uses the specific drug for the specific receptor to regulate the excitation of suppression of affected neurons.[59] However, some concerns have been raised in the previous study of CNO as a specific drug.[54] First, a small amount of CNO is metabolized to clozapine. Second, compared with clozapine, CNO has less binding capacity for the DREADD receptor and passes the blood-brain barrier less. To compensate for these concerns, more specific DREADD receptor agonists such as DREADD 21 was developed.[65] In our study, clozapine control experiments were performed, which showed an increase in PPI in both control (*Irsp53*$^{fl/fl}$) and *Emx1-Cre;Irsp53*$^{fl/fl}$ mice (supplementary figure S5). In addition, there was no difference in PPI between control and *Emx1-Cre;Irsp53*$^{fl/fl}$ mice treated CNO without AAV injection (supplementary figure S4). In the results of LC/MS, a 5-HT difference between control and *Emx1-Cre;Irsp53*$^{fl/fl}$ mice was observed, and there was no difference in the neurotransmitter between CNO and vehicle in WT mice (supplementary figure S5). Based on these results, the chemogenetic effect of CNO on DREADD receptor can be considered to induce the ACC-MDT circuit inhibition. As our hypothesis, it may be suggested that reducing the increased excitability of ACC layer VI cortical neurons projecting to MDT can improve the reduced PPI.

IRSp53 has been implicated in various neuropsychiatric disorders, including schizophrenia,[39,40] autism spectrum disorders,[41–43,45] and attention-deficit/hyperactivity disorder.[44,45] Whether the decreased PPI in IRSp53-mutant mice is associated with the pathophysiology of these diseases remains unclear. However, there is significant overlap between the disorders related with PPI alterations and IRSp53 mutations, including schizophrenia and autism spectrum disorders.[1,3–5,39–43] Therefore, the reduced PPI observed in our study might be a useful biomarker for the diagnosis and treatment of IRSp53-related disorders, as suggested previously.[2]

In conclusion, our study reveals a novel role of IRSp53 in the maintenance of normal PPI and the critical role of MDT neurons and the ACC-MDT pathway in the regulation of PPI.

Supplementary Material

Supplementary material is available at *Schizophrenia Bulletin*.

Funding

This study was supported by the Institute for Basic Science (IBS-R002-D1 to E.K.) and by an intramural research of the National Center for Mental Health in Republic of Korea (R2020-C to Y.K.).

Acknowledgments

pAAV-hSyn-hM4D(Gi)-mCherry, pAAV-hSyn-DIO-HA-hM3D(Gq)-IRES-mCitrine, and pAAV-hSyn-DIO-HA-hM4D(Gi)-IRES-mCitrine were a gift from Dr. Bryan Roth (Addgene viral prep # 50475-AAVrg; # 50454-AAV8; # 50454-AAV8). pAAV-Ef1a-mCherry-IRES-Cre was a gift from Karl Deisseroth (Addgene plasmid # 55632-AAV8). The authors declare that they have no competing financial interests.

References

1. Braff DL, Geyer MA, Swerdlow NR. Human studies of prepulse inhibition of startle: normal subjects, patient groups, and pharmacological studies. *Psychopharmacology (Berl)*. 2001;156(2-3):234–258.
2. Swerdlow NR, Braff DL, Geyer MA. Sensorimotor gating of the startle reflex: what we said 25 years ago, what has happened since then, and what comes next. *J Psychopharmacol*. 2016;30(11):1072–1081.
3. Perry W, Minassian A, Lopez B, Maron L, Lincoln A. Sensorimotor gating deficits in adults with autism. *Biol Psychiatry*. 2007;61(4):482–486.
4. Kohl S, Heekeren K, Klosterkötter J, Kuhn J. Prepulse inhibition in psychiatric disorders–apart from schizophrenia. *J Psychiatr Res*. 2013;47(4):445–452.
5. Braff DL. Prepulse inhibition of the startle reflex: a window on the brain in schizophrenia. *Curr Top Behav Neurosci*. 2010;4:349–371.
6. Swerdlow NR, Paulsen J, Braff DL, Butters N, Geyer MA, Swenson MR. Impaired prepulse inhibition of acoustic and tactile startle response in patients with Huntington's disease. *J Neurol Neurosurg Psychiatry*. 1995;58(2):192–200.
7. Hejl AM, Glenthøj B, Mackeprang T, Hemmingsen R, Waldemar G. Prepulse inhibition in patients with Alzheimer's disease. *Neurobiol Aging*. 2004;25(8):1045–1050.
8. Swerdlow NR, Geyer MA, Braff DL. Neural circuit regulation of prepulse inhibition of startle in the rat: current knowledge and future challenges. *Psychopharmacology (Berl)*. 2001;156(2-3):194–215.

9. Fendt M, Li L, Yeomans JS. Brain stem circuits mediating prepulse inhibition of the startle reflex. *Psychopharmacology (Berl)*. 2001;156(2-3):216–224.
10. Geyer MA, McIlwain KL, Paylor R. Mouse genetic models for prepulse inhibition: an early review. *Mol Psychiatry*. 2002;7(10):1039–1053.
11. Powell SB, Zhou X, Geyer MA. Prepulse inhibition and genetic mouse models of schizophrenia. *Behav Brain Res*. 2009;204(2):282–294.
12. Veeraragavan S, Graham D, Bui N, Yuva-Paylor LA, Wess J, Paylor R. Genetic reduction of muscarinic M4 receptor modulates analgesic response and acoustic startle response in a mouse model of fragile X syndrome (FXS). *Behav Brain Res*. 2012;228(1):1–8.
13. Swerdlow NR, Weber M, Qu Y, Light GA, Braff DL. Realistic expectations of prepulse inhibition in translational models for schizophrenia research. *Psychopharmacology (Berl)*. 2008;199(3):331–388.
14. Azzopardi E, Louttit AG, DeOliveira C, Laviolette SR, Schmid S. The role of cholinergic midbrain neurons in startle and prepulse inhibition. *J Neurosci*. 2018;38(41):8798–8808.
15. Dugué GP, Lörincz ML, Lottem E, Audero E, Matias S, et al. Optogenetic recruitment of dorsal raphe serotonergic neurons acutely decreases mechanosensory responsivity in behaving mice. *PLoS ONE* 2014;9(8):e105941. doi:10.1371/journal.pone.0105941.
16. Fulcher N, Azzopardi E, De Oliveira C, et al. Deciphering midbrain mechanisms underlying prepulse inhibition of startle. *Prog Neurobiol*. 2020;185:101734.
17. Mitchell AS. The mediodorsal thalamus as a higher order thalamic relay nucleus important for learning and decision-making. *Neurosci Biobehav Rev*. 2015;54:76–88.
18. Mitchell AS, Chakraborty S. What does the mediodorsal thalamus do? *Front Syst Neurosci*. 2013;7:37.
19. Heidbreder CA, Groenewegen HJ. The medial prefrontal cortex in the rat: evidence for a dorso-ventral distinction based upon functional and anatomical characteristics. *Neurosci Biobehav Rev*. 2003;27(6):555–579.
20. Divac I, Mogensen J, Petrovic-Minic B, Zilles K, Regidor J. Cortical projections of the thalamic mediodorsal nucleus in the rat. Definition of the prefrontal cortex. *Acta Neurobiol Exp (Wars)*. 1993;53(2):425–429.
21. Kuroda M, Yokofujita J, Murakami K. An ultrastructural study of the neural circuit between the prefrontal cortex and the mediodorsal nucleus of the thalamus. *Prog Neurobiol*. 1998;54(4):417–458.
22. Delevich K, Tucciarone J, Huang ZJ, Li B. The mediodorsal thalamus drives feedforward inhibition in the anterior cingulate cortex via parvalbumin interneurons. *J Neurosci*. 2015;35(14):5743–5753.
23. Parnaudeau S, O'Neill PK, Bolkan SS, et al. Inhibition of mediodorsal thalamus disrupts thalamofrontal connectivity and cognition. *Neuron* 2013;77(6):1151–1162.
24. Parnaudeau S, Taylor K, Bolkan SS, Ward RD, Balsam PD, Kellendonk C. Mediodorsal thalamus hypofunction impairs flexible goal-directed behavior. *Biol Psychiatry*. 2015;77(5):445–453.
25. Bolkan SS, Stujenske JM, Parnaudeau S, et al. Thalamic projections sustain prefrontal activity during working memory maintenance. *Nat Neurosci*. 2017;20(7):987–996.
26. Mitelman SA, Byne W, Kemether EM, Hazlett EA, Buchsbaum MS. Metabolic disconnection between the mediodorsal nucleus of the thalamus and cortical Brodmann's areas of the left hemisphere in schizophrenia. *Am J Psychiatry*. 2005;162(9):1733–1735.
27. Seidman LJ, Yurgelun-Todd D, Kremen WS, et al. Relationship of prefrontal and temporal lobe MRI measures to neuropsychological performance in chronic schizophrenia. *Biol Psychiatry*. 1994;35(4):235–246.
28. Ray JP, Price JL. The organization of the thalamocortical connections of the mediodorsal thalamic nucleus in the rat, related to the ventral forebrain-prefrontal cortex topography. *J Comp Neurol*. 1992;323(2):167–197.
29. Pirot S, Jay TM, Glowinski J, Thierry AM. Anatomical and electrophysiological evidence for an excitatory amino acid pathway from the thalamic mediodorsal nucleus to the prefrontal cortex in the rat. *Eur J Neurosci*. 1994;6(7):1225–1234.
30. Groenewegen HJ. Organization of the afferent connections of the mediodorsal thalamic nucleus in the rat, related to the mediodorsal-prefrontal topography. *Neuroscience* 1988;24(2):379–431.
31. Burette AC, Park H, Weinberg RJ. Postsynaptic distribution of IRSp53 in spiny excitatory and inhibitory neurons. *J Comp Neurol*. 2014;522(9):2164–2178.
32. Kang J, Park H, Kim E. IRSp53/BAIAP2 in dendritic spine development, NMDA receptor regulation, and psychiatric disorders. *Neuropharmacology* 2016;100:27–39.
33. Sheng M, Hoogenraad CC. The postsynaptic architecture of excitatory synapses: a more quantitative view. *Annu Rev Biochem*. 2007;76:823–847.
34. Sheng M, Sala C. PDZ domains and the organization of supramolecular complexes. *Annu Rev Neurosci*. 2001;24:1–29.
35. Sheng M, Kim E. The postsynaptic organization of synapses. *Cold Spring Harb Perspect Biol*. 2011;3(12):a005678.doi:10.1101/cshperspect.a005678.
36. Choi J, Ko J, Racz B, et al. Regulation of dendritic spine morphogenesis by insulin receptor substrate 53, a downstream effector of Rac1 and Cdc42 small GTPases. *J Neurosci*. 2005;25(4):869–879.
37. Soltau M, Berhörster K, Kindler S, Buck F, Richter D, Kreienkamp HJ. Insulin receptor substrate of 53 kDa links postsynaptic shank to PSD-95. *J Neurochem*. 2004;90(3):659–665.
38. Miki H, Yamaguchi H, Suetsugu S, Takenawa T. IRSp53 is an essential intermediate between Rac and WAVE in the regulation of membrane ruffling. *Nature* 2000;408(6813):732–735.
39. Fromer M, Pocklington AJ, Kavanagh DH, et al. De novo mutations in schizophrenia implicate synaptic networks. *Nature* 2014;506(7487):179–184.
40. Purcell SM, Moran JL, Fromer M, et al. A polygenic burden of rare disruptive mutations in schizophrenia. *Nature* 2014;506(7487):185–190.
41. Celestino-Soper PB, Shaw CA, Sanders SJ, et al. Use of array CGH to detect exonic copy number variants throughout the genome in autism families detects a novel deletion in TMLHE. *Hum Mol Genet*. 2011;20(22):4360–4370.
42. Levy D, Ronemus M, Yamrom B, et al. Rare de novo and transmitted copy-number variation in autistic spectrum disorders. *Neuron* 2011;70(5):886–897.
43. Toma C, Hervás A, Balmaña N, et al. Association study of six candidate genes asymmetrically expressed in the two cerebral hemispheres suggests the involvement of BAIAP2 in autism. *J Psychiatr Res*. 2011;45(2):280–282.
44. Liu L, Sun L, Li ZH, et al. BAIAP2 exhibits association to childhood ADHD especially predominantly inattentive subtype in Chinese Han subjects. *Behav Brain Funct*. 2013;9:48.

45. Ribasés M, Bosch R, Hervás A, et al. Case-control study of six genes asymmetrically expressed in the two cerebral hemispheres: association of BAIAP2 with attention-deficit/hyperactivity disorder. *Biol Psychiatry*. 2009;66(10):926–934.
46. Kim MH, Choi J, Yang J, et al. Enhanced NMDA receptor-mediated synaptic transmission, enhanced long-term potentiation, and impaired learning and memory in mice lacking IRSp53. *J Neurosci*. 2009;29(5):1586–1595.
47. Chung W, Choi SY, Lee E, et al. Social deficits in IRSp53 mutant mice improved by NMDAR and mGluR5 suppression. *Nat Neurosci*. 2015;18(3):435–443.
48. Gorski JA, Talley T, Qiu M, Puelles L, Rubenstein JL, Jones KR. Cortical excitatory neurons and glia, but not GABAergic neurons, are produced in the Emx1-expressing lineage. *J Neurosci*. 2002;22(15):6309–6314.
49. Kim Y, Noh YW, Kim K, Yang E, Kim H, Kim E. IRSp53 deletion in glutamatergic and GABAergic neurons and in male and female mice leads to distinct electrophysiological and behavioral phenotypes. *Front Cell Neurosci*. 2020;14:23.
50. Ledergerber D, Larkum ME. Properties of layer 6 pyramidal neuron apical dendrites. *J Neurosci*. 2010;30(39):13031–13044.
51. Yi F, Danko T, Botelho SC, et al. Autism-associated SHANK3 haploinsufficiency causes Ih channelopathy in human neurons. *Science* 2016;352(6286):aaf2669.
52. Armbruster BN, Li X, Pausch MH, Herlitze S, Roth BL. Evolving the lock to fit the key to create a family of G protein-coupled receptors potently activated by an inert ligand. *Proc Natl Acad Sci U S A*. 2007;104(12):5163–5168.
53. Zhu H, Roth BL. DREADD: a chemogenetic GPCR signaling platform. *Int J Neuropsychopharmacol*. 2015;18(1):pyu007.
54. Gomez JL, Bonaventura J, Lesniak W, et al. Chemogenetics revealed: DREADD occupancy and activation via converted clozapine. *Science* 2017;357(6350):503–507.
55. Brown SP, Mathur BN, Olsen SR, Luppi PH, Bickford ME, Citri A. New breakthroughs in understanding the role of functional interactions between the neocortex and the claustrum. *J Neurosci*. 2017;37(45):10877–10881.
56. Jackson J, Karnani MM, Zemelman BV, Burdakov D, Lee AK. Inhibitory control of prefrontal cortex by the Claustrum. *Neuron* 2018;99(5):1029–1039 e1024.
57. Stachniak TJ, Ghosh A, Sternson SM. Chemogenetic synaptic silencing of neural circuits localizes a hypothalamus→midbrain pathway for feeding behavior. *Neuron* 2014;82(4):797–808.
58. Mahler SV, Vazey EM, Beckley JT, et al. Designer receptors show role for ventral pallidum input to ventral tegmental area in cocaine seeking. *Nat Neurosci*. 2014;17(4):577–585.
59. Roth BL. DREADDs for neuroscientists. *Neuron* 2016;89(4):683–694.
60. Wegner AM, Nebhan CA, Hu L, et al. N-wasp and the arp2/3 complex are critical regulators of actin in the development of dendritic spines and synapses. *J Biol Chem*. 2008;283(23):15912–15920.
61. Rácz B, Weinberg RJ. Organization of the Arp2/3 complex in hippocampal spines. *J Neurosci*. 2008;28(22):5654–5659.
62. Kim IH, Rossi MA, Aryal DK, et al. Spine pruning drives antipsychotic-sensitive locomotion via circuit control of striatal dopamine. *Nat Neurosci*. 2015;18(6):883–891.
63. Kim IH, Racz B, Wang H, et al. Disruption of Arp2/3 results in asymmetric structural plasticity of dendritic spines and progressive synaptic and behavioral abnormalities. *J Neurosci*. 2013;33(14):6081–6092.
64. Ray JP, Russchen FT, Fuller TA, Price JL. Sources of presumptive glutamatergic/aspartatergic afferents to the mediodorsal nucleus of the thalamus in the rat. *J Comp Neurol*. 1992;320(4):435–456.
65. Thompson KJ, Khajehali E, Bradley SJ, et al. DREADD agonist 21 is an effective agonist for muscarinic-based DREADDs in vitro and in vivo. *ACS Pharmacol Transl Sci*. 2018;1(1):61–72.